Three-Dimensional Analysis of the Ideal Entry Point for Sacral Alar Iliac Screws

Noriyuki Watanabe[1,2], Tomoyuki Takigawa[1,3], Koji Uotani[1,4],
Yoshiaki Oda[1], Haruo Misawa[1], Masato Tanaka[1,4], Toshifumi Ozaki[1]

[1]Department of Orthopaedic Surgery, Okayama University Hospital, Okayama, Japan
[2]Department of Orthopaedic Surgery, National Hospital Organization Iwakuni Clinical Center, Yamaguchi, Japan
[3]Department of Orthopaedic Surgery, Kobe Red Cross Hospital, Kobe, Japan
[4]Department of Orthopaedic Surgery, Okayama Rosai Hospital, Okayama, Japan

Study Design: This is a virtual three-dimensional (3D) imaging study examining computed tomography (CT) data to investigate instrumentation placement.

Purpose: In this study, we aim to clarify the ideal entry point and trajectory of the sacral alar iliac (SAI) screw in relationship to the dorsal foramen at S1 and the respective nerve root.

Overview of Literature: To the best of our knowledge, there is yet no detailed 3D imaging study on the ideal entry point of the SAI screw. Despite the evidence suggesting that the dorsal foramen at S1 is a landmark on the sacrum, the S1 nerve root disruption is a general concern during the insertion of SAI screws. No other study has been published examining the nerve root location at the S1and SAI screw insertions.

Methods: Preoperative CT data from 26 patients pertaining to adult spinal deformities were investigated in this study. We applied a 3D image processing method for a detailed investigation. Virtual cylinders were used to mimic SAI screws. These were placed to penetrate the sacral iliac joint without violating the other cortex. We then assessed the trajectory of the longest SAI screw and the ideal entry point of SAI using a color mapping method on the surface of the sacrum. We measured the location of the nerve root at S1 in relation to the foramen at S1 and the sacral surface.

Results: As per the results of our color mapping, it was determined that areas that received high scores are located medially and caudally to the dorsal foramen of S1. The mean angle between a horizontal line and a line connecting the medial edge of the foramen and nerve root at S1 was 93.5°. The mean distances from the dorsal medial edge of the foramen and sacral surface to S1 nerve root were 21.8 mm and 13.9 mm, respectively.

Conclusions: The ideal entry point of the SAI screw is located medially and caudally to the S1 dorsal foramen based on 3D digital mapping. It is also shown that this entry point spares the S1 nerve root from possible iatrogenic injuries.

Keywords: S1 nerve root; S1 dorsal foramen; Adult spinal deformity; Sacral alar iliac screw; Ideal entry point

Introduction

The sacral alar iliac (SAI) screw technique has been introduced and popularized by O'Brien et al. [1]. Nowadays, SAI screws are applied in a variety of clinical settings. The SAI screw utilizes the sacral alar trajectory screw and is placed across the sacroiliac (SI) joint into the ilium [1-4]. Several authors have already reported that the SAI screw technique can minimize the implant prominence and soft tissue dissection [5-7]. Additionally, the SAI screw can be placed through percutaneous and minimally invasive methods [8,9]. O'Brien et al. [1] reported the mean length of the SAI screw and the mean angle of the trajectory in the lateral and caudal directions in Caucasian cadavers subject to the condition that the entry point was 1 mm inferior and 1 mm lateral to the foramen at S1. Chang et al. [5] reported that the mean starting point in S2 was 25 mm caudal to the superior endplate of S1 and 22 mm lateral to the sacral midline based on the ideal trajectory in the computed tomography (CT) radiographic analysis of Caucasians. Zhu et al. [6] reported the mean length of the SAI screw and the mean angle of the trajectory subject to the condition that entry point was 1 mm inferior and 1 mm lateral to S1 foramen in CT radiographic analysis of Chinese. In these reports, the most commonly used entry point was 1 mm inferior and 1 mm lateral to the foramen at S1. Trajectories and lengths of the SAI screw are based on these predecided entry points. To our knowledge, there is no detailed three-dimensional (3D) imaging study on the ideal entry point of the SAI screw. Thus, in this study, we used a 3D medical image processing software for a more detailed investigation. Although the dorsal neural foramen at S1 is a landmark on the sacrum for SAI screw insertion, nerve root damage during the insertion of SAI screws remains to be a general concern. Thus, this study aimed to clarify the ideal entry point and trajectory of SAI screw in relationship with the dorsal foramen and nerve root at S1.

Materials and Methods

This study was performed according to the principles described in the Declaration of Helsinki and was approved by the Institutional Ethics Review Board of Okayama University Hospital (approval no., 1702-007). We applied an opt-out method to obtain consent on this study because this was a retrospective study and analysis used anony-mous clinical data which were obtained after each patient agreed to surgical treatment according to written consent.

1. Subjects

Preoperative CT data for adult spinal deformity from 32 patients were used. In total, 13 males and 19 females were examined. The average age of males and females were 59.7 years and 61.5 years, respectively, at the time of the CT examination. The average height and weight were 161.8 cm and 63.7 kg in males and 148.8 cm and 47.5 kg in females, respectively. No patient had metabolic bone disease, previous history of pelvic fracture, or pelvic surgery.

2. Computed tomography reconstruction and radiographic parameters

A 64-slice CT scanner (Siemens Healthineers, Erlangen, Germany) was used to scan the entire pelvis with a layer thickness of 1 mm. The CT scan data (Digital Image Communications in Medicine format) of each patient was imported into the software Mimics (ver. 17.0; Materialise, Leuven, Belgium) for a 3D interactive viewing and manipulation. The threshold Hounsfield unit value needed to create a bone model was set at "226 to maximum." After the 3D digital image was reconstructed, virtual cylinders (diameters of 8 mm, 9 mm, and 10 mm) were drawn to mimic the SAI screws inserted from the right sacrum to the right ilium (Fig. 1). In this study, the SAI screw was placed in such a way to penetrate the SI joint without violating the cortex. Furthermore, its tip was designed to be localized at the supra-acetabular region without causing damage to the contralateral cortex.

We then assessed the maximum length of SAI screws with diameters equal to 8 mm, 9 mm, and 10 mm. We also measured the trajectories of the SAI screws with these maximum lengths in the transverse and sagittal planes and distance between the entry point of the longest SAI screw and the posterior foramen at S1.

To assess the ideal entry point of SAI, we opted to apply a color mapping method on the surface of the sacrum. Firstly, we created a virtual grid spacing of 2.5 mm at the origin at the center of the S1 posterior foramen. Secondly, we applied virtual screws with various lengths from each grid intersection. We then allocated the following point grades when the virtual screw remained within the bone depending on the screw length: 5 points, maximum

length; 3 points, maximum minus 5 mm; and 1 point, maximum minus 10 mm length. Each square comprised 4 quadrants and was scored with the average point of 4 entry points. We repeated this measurement and summed the square points of all patients. Lastly, we created a color mapping on the surface of the sacrum depending on the screw size (8 mm, 9 mm, and 10 mm). The calculation of
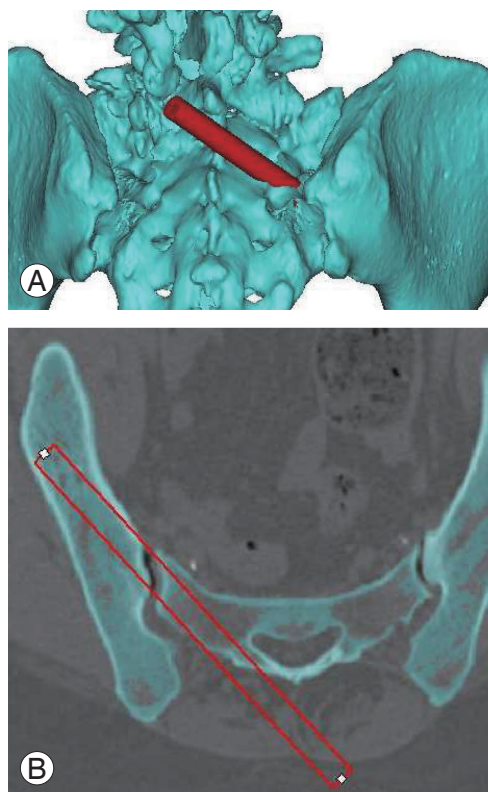
color mapping was made automatically using Excel 2013 (Microsoft Corp., Redmond, WA, USA), with red denoting the maximum and green the minimum.

3. Relationship between S1 nerve root and the dorsal foramen

To analyze the relationship between the nerve root at S1 and the dorsal foramen, we selected the axial CT slice, in which the neural foramen at S1 appeared to have the largest width. We then defined the following three angles: angle S, an angle between a horizontal line and a tangential line of the foramen at S1; angle A, an angle between a horizontal line and a line connecting the medial edge of the foramen at S1 and the alar; and angle R, angle between a horizontal line and a line connecting the medial edge of the foramen at S1 and the lateral edge of the nerve root at S1 (Fig. 2). We measured the distance from the dorsal medial edge of the foramen to the nerve root (L) at S1 and the distance from sacral surface to the nerve root (M) at S1 as L×sin (R-S) (Fig. 2B). All results were represented as mean and standard deviation (SD).

Results

The mean±SD maximum lengths of SAI screws with diameters of 8 mm, 9 mm, and 10 mm were 122.1±2.4 mm, 118.9±2.8 mm, and 116.6±3.0 mm in males and 112.1±3.4 mm, 105.8±3.7 mm, and 103.9±4.6 mm in females, respectively. The trajectories of the longest SAI screw are shown in Fig. 3. The mean±SD angles in the transverse plane with diameters equal to 8 mm, 9 mm, and 10 mm
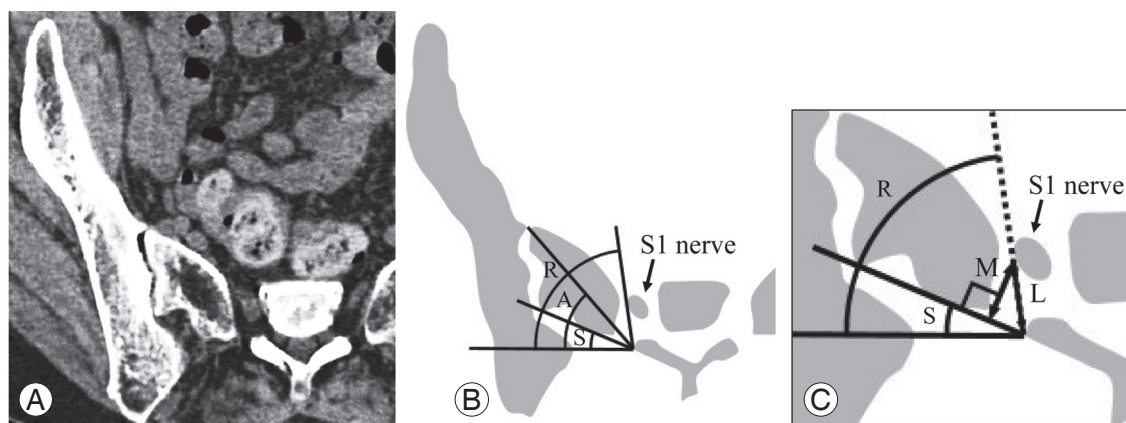

Fig. 1. Three-dimensional **(A)** and axial **(B)** computed tomography image of sacropelvic and cylinder.

Fig. 2. (A–C) S1 nerve root location in relationship with S1 dorsal foramen. S: angle between tangential line of S1 dorsal foramen and horizontal line; A: angle between medial S1 foramen to the alar and horizontal line; R: angle between medial S1 foramen to the lateral S1 nerve root and horizontal line; L: distance from dorsal medial foramen to S1 nerve root; M: distance from sacral surface to S1 nerve root; M=L×sin (R-S).
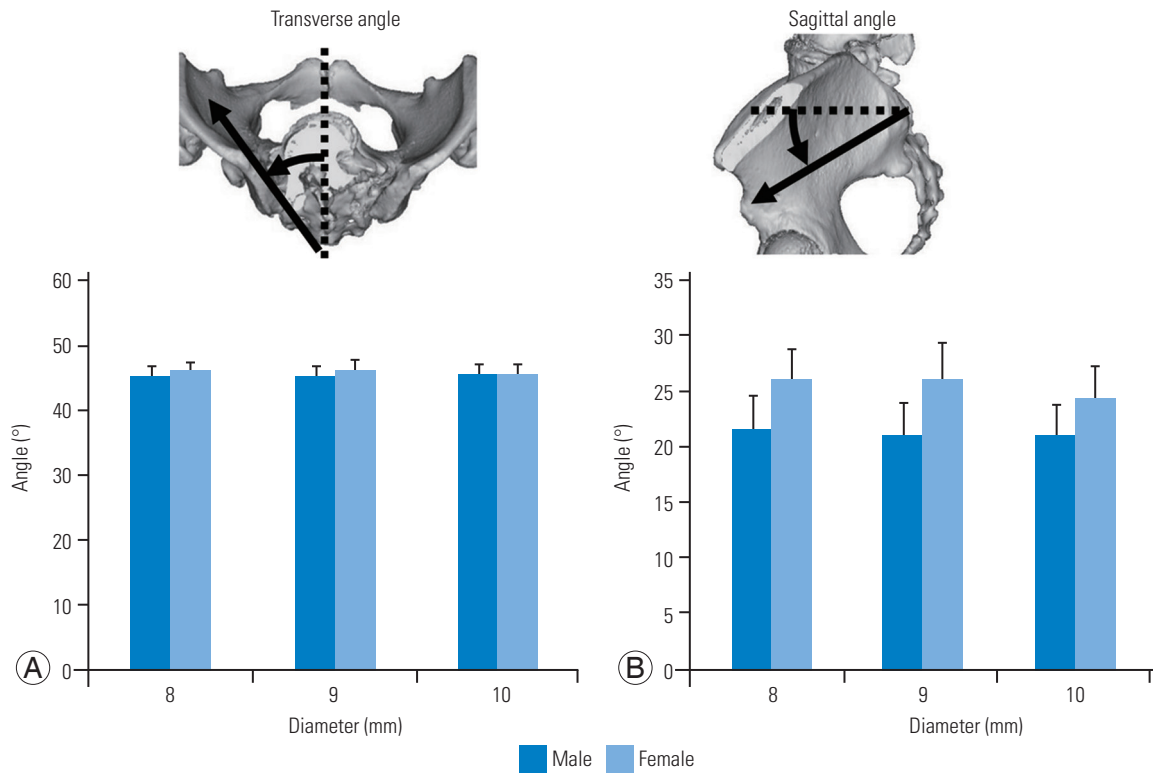
Fig. 3. The mean angle of SAI screw trajectory in transverse **(A)** and sagittal **(B)** plane. Bars represent standard deviations.

in males were 45.2°±1.7°, 45.4°±1.6°, and 45.6°±1.6°, respectively; meanwhile, those in females were 45.9°±1.6°, 46.1°±1.8°, and 45.6°±1.7°, respectively. The mean±SD angles in the sagittal plane with diameters of 8 mm, 9 mm, and 10 mm in males were 21.7°±3.0°, 21.1°±2.8°, and 20.8°±2.9°, respectively. Moreover, those in females were 26.0°±2.9°, 26.1°±3.1°, and 24.2°±3.1°, respectively. These results indicate that the mean trajectory in females was more lateral in the transverse plane and more caudal in the sagittal plane than those in males.

The entry points of the longest SAI screws were located medially and caudally to the posterior foramen at S1 in all cases. The mean distances of the entry points of the longest SAI screws with diameter of 8 mm, 9 mm, and 10 mm from the posterior foramen at S1 were 6.9 mm, 5.5 mm, and 4.1 mm in the medial direction and 2.8 mm, 2.6 mm, and 2.6 mm in the caudal direction in males, respectively. Those in females were 5.0 mm, 4.4 mm, and 3.9 mm in the medial direction and 1.8 mm, 2.1 mm, and 2.5 mm in the caudal direction, respectively. Color mapping results showed that high scored areas are located medially and caudally to the posterior foramen at S1 in all diameters (Fig. 4). The means of the angles S, A, and R were

20.9°, 56.4°, and 93.5°, respectively (Fig. 5). The means L and M were 21.8 mm and 13.9 mm, respectively (Fig. 6).

Discussion

Pelvic fixation has been commonly used to correct severe scoliosis and/or kyphosis observed in patients with various neuromuscular conditions and adult spinal deformity [10,11]. However, long spinal fusion to the sacrum is still a challenging procedure. Traditional pelvic fixations include Galveston, sacral, and iliac screw techniques [12-16]. These conventional techniques have several problems related to their biomechanical strengths and implant prominence [15,17-20]. The Galveston technique is one of the most popular methods, but this often requires complex and 3D rod bending. However, compared with the Galveston technique, the combined technique using sacral and iliac screws allows easier implant placements [17,21,22]. But, the strength of the sacral screw is not satisfactory as implant failure and loss of correction may occur [14,15]. The iliac screw technique is one of the most commonly used techniques for pelvic fixation and provides better pull-out strength compared with the Galveston and sacral
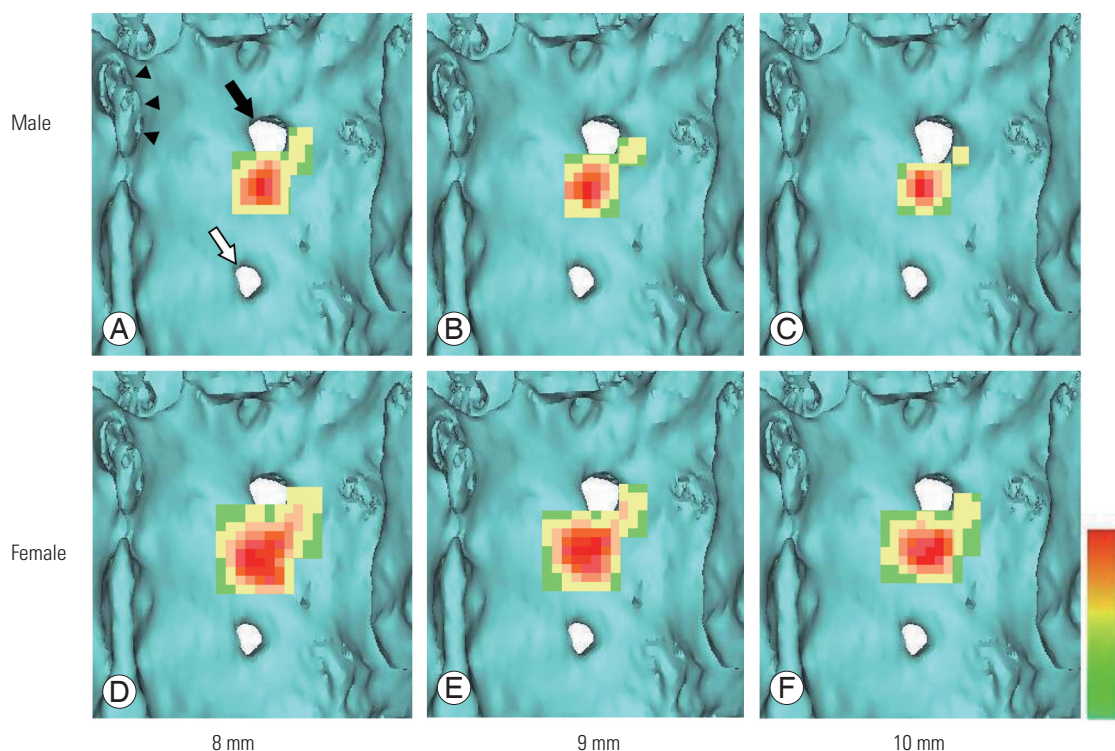
Fig. 4. (A–F) Color mapping of entry point depending on the length of screw and sex. Black arrow is right S1 dorsal foramen, white arrow is right S2 foramen, and arrowheads are S1 spinous process. Red is the highest and the green is the lowest score. The highest area locates medial and caudal to S1 dorsal foramen in all cases.
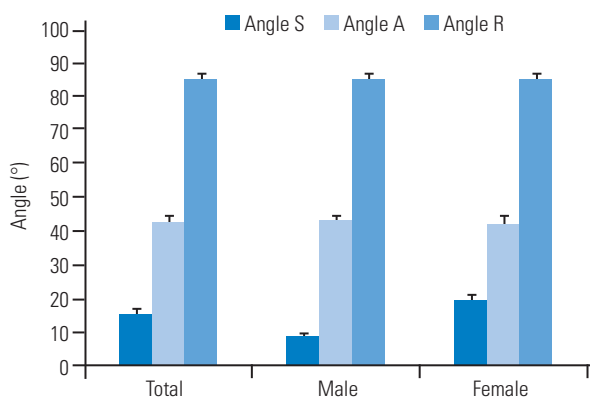

Fig. 5. The mean of angle S, A, and R. Bars represent standard deviations. S: angle between tangential line of S1 dorsal foramen and horizontal line; A: angle between medial S1 foramen to the alar and horizontal line; R: angle between medial S1 foramen to the lateral S1 nerve root and horizontal line.
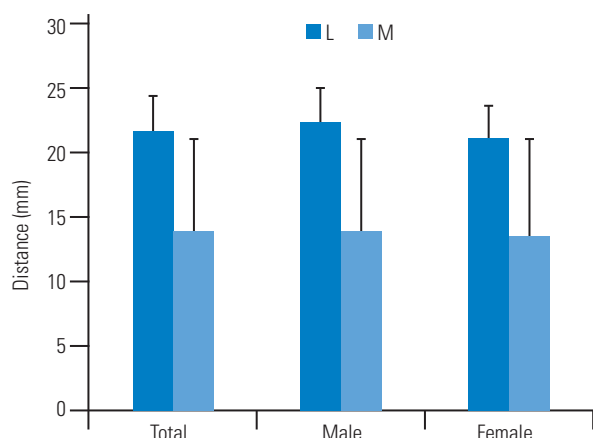

Fig. 6. The mean of L and M. L is distance from S1 dorsal medial edge of foramen to S1 nerve root, and M is distance from sacral surface to S1 nerve root. Bars represent standard deviations.

screw techniques [17]. Several authors showed that additional iliac screws may be effective in enhancing fusion rates at the lumbosacral junction [19,20,23,24]. However, implant prominence over the iliac crest and wide soft tissue dissection were reported in the case of the iliac screw technique [20]. These may increase the possibility of deep wound infection and poor wound healing. Tsuchiya et

al. [19] reported that 23 of 67 patients treated for adult spinal deformity with iliac screws required iliac screw removal for periods which lasted up to 5 years because of implant prominence. The SAI screw technique has been introduced to overcome these problems [1]. Typically, SAI screws are inserted from the surface of the sacrum, thus minimizing the risk of implant prominence.

Several authors reported their findings on entry point, trajectory, and on the lengths of SAI screws [1,5,6]. For example, O'Brien et al. [1] showed that the mean length of SAI screws was 84 mm, and the mean angle of trajectory were 40° in the lateral and 33° in the caudal directions with the entry point being 1 mm in the inferior and 1 mm in the lateral directions to the S1 foramen in Caucasian cadavers. Chang et al. [5] reported that the mean starting point in S2 was 25 mm caudally to the superior endplate of S1 and 22 mm laterally to the sacral midline based on the ideal trajectory. The mean length of SAI screws was 105 mm, and the mean trajectory angle was 40° in the lateral and 40° in the caudal directions in the CT radiographic analysis of Caucasians. Zhu et al. [6] have also showed that the mean length of SAI screws was 118 mm, and the mean angles were 36° in the lateral and 32° in the caudal directions subject to the condition that entry point was 1 mm inferior and 1 mm lateral to the S1 foramen in CT radiographic analysis of Chinese patients. Our results about screw length correspond with the previous reports. Conversely, the angle of the screw trajectory in the transverse plane in our study (45°–47°) was larger, and that in the sagittal plane was smaller (20°–22° in males and 24°–26° in females) than those reported previously. We assume that these discrepancies were attributed to the difference of the setting of the screw entry point. Most of the previous manuscripts on SAI screws used the entry point located just laterally and caudally to the S1 neural foramen. However, as shown in the color mapping results in this study, the ideal entry point of the SAI screw was located medially and more caudally to the neural foramen at S1. Because the tip of SAI screw is convergent at the supra-acetabular region, medial and caudal movements of the entry point require large and small angles in the transverse and sagittal planes, respectively.

The SAI screw technique requires 3D recognition from the sacrum to the ilium through the SI joint in order to avoid damage to the cortex. Thus, we believe that the screw diameter should be considered to identify the screw entry point and trajectory. O'Brien et al. [25] showed that there were no significant differences in the strengths of fixation among the three types of SAI screws, namely, those with lengths equal to (1) 65 mm in the tricortical purchase, (2) 80 mm in the tricortical purchase, and (3) 50 mm in the quad-cortical purchase. These results indicate that anchoring the SI joint is the most important to achieve an adequate biomechanical strength. In our study,

we designed the location of the cylinder which penetrated the SI joint without violating the cortex.

Previous papers and our results showed that the entry point of SAI had a relatively wide range. In fact, Wu et al. [26] reported the feasibility of SAI screws from S1 to S4. Our color mapping results as regards the entry point of SAI screw demonstrated that the high scored areas (i.e., the ideal entry point) were located medially and caudally to the posterior foramen at S1. When the SAI screw was inserted from the medial to neural foramen at S1, the nerve root at S1 may be critical. In this study, we also identified the nerve root location at S1 in relationship to the respective dorsal foramen. The mean of the angle R, which is an angle between the horizontal line and the line which connected the medial edge of the foramen at S1 and the lateral edge of the respective nerve root, was approximately 90°. This result shows that the lateral edge of the nerve root at S1 is located just under the medial edge of the dorsal foramen at S1. The risk of the nerve root damage at S1 is the highest at the insertion point because the transverse angle of SAI screw in this study was approximately 45° and the screw tip departed from the nerve root at S1 as it penetrated deeper regions. However, the mean distance from the dorsal medial edge of the foramen to nerve root at S1 and the mean distances from sacral surface to S1 nerve root were 21.8 mm and 13.9 mm, respectively. These results indicate that even a thick SAI screw, such as 10 mm in diameter (5 mm in radius), can be inserted from the dorsal foramen at S1 without damaging the respective nerve root. Because the medial border of the foramen at S1 is prominent and steep against the lateral trajectory, the lateral border of the foramen at S1 is more convenient for the application of the SAI screw. When connecting the L5 screw, as the location of the SAI screw shifts more toward the medial direction, it becomes more difficult to connect the rod. Because the location of the nerve root at S1 was investigated only at the center of the neural foramen at S1, the safety margin caudal to the foramen at S1 was not guaranteed for this study. Clinically, the insertion point of the SAI screw should be decided based on these balances.

The major limitation of this study is attributed to the fact that the results were obtained by virtual cylinders in small sample sizes and were not compared with the actual clinical results. This study was only based on virtual image analysis. Thus, prospective clinical research is required to validate this study.

Conclusions

The ideal entry point of SAI screw is located medially and caudally to the dorsal foramen at S1 based on 3D digital mapping. This finding also shows that this entry point spares the S1 nerve root from possible iatrogenic injuries.

Conflict of Interest

No potential conflict of interest relevant to this article was reported.

Author Contributions

Data acquisition: NW; Analysis of data: NW, TT; drafting of the manuscript: NW, TT; conception and design: TT, MT; critical revision KU, YO, HM, MT, TO; and supervision MT, TO.

References

1. O'Brien JR, Yu WD, Bhatnagar R, Sponseller P, Kebaish KM. An anatomic study of the S2 iliac technique for lumbopelvic screw placement. Spine (Phila Pa 1976) 2009;34:E439-42.

2. Matteini LE, Kebaish KM, Volk WR, Bergin PF, Yu WD, O'Brien JR. An S-2 alar iliac pelvic fixation. Technical note. Neurosurg Focus 2010;28:E13.

3. Nottmeier EW, Pirris SM, Balseiro S, Fenton D. Three-dimensional image-guided placement of S2 alar screws to adjunct or salvage lumbosacral fixation. Spine J 2010;10:595-601.

4. Mattei TA, Fassett DR. Low-profile pelvic fixation with sacral alar-iliac screws. Acta Neurochir (Wien) 2013;155:293-7.

5. Chang TL, Sponseller PD, Kebaish KM, Fishman EK. Low profile pelvic fixation: anatomic parameters for sacral alar-iliac fixation versus traditional iliac fixation. Spine (Phila Pa 1976) 2009;34:436-40.

6. Zhu F, Bao HD, Yuan S, et al. Posterior second sacral alar iliac screw insertion: anatomic study in a Chinese population. Eur Spine J 2013;22:1683-9.

7. Sponseller PD, Zimmerman RM, Ko PS, et al. Low profile pelvic fixation with the sacral alar iliac technique in the pediatric population improves results at two-year minimum follow-up. Spine (Phila Pa 1976) 2010;35:1887-92.

8. Martin CT, Witham TF, Kebaish KM. Sacropelvic fixation: two case reports of a new percutaneous technique. Spine (Phila Pa 1976) 2011;36:E618-21.

9. O'Brien JR, Matteini L, Yu WD, Kebaish KM. Feasibility of minimally invasive sacropelvic fixation: percutaneous S2 alar iliac fixation. Spine (Phila Pa 1976) 2010;35:460-4.

10. Weistroffer JK, Perra JH, Lonstein JE, et al. Complications in long fusions to the sacrum for adult scoliosis: minimum five-year analysis of fifty patients. Spine (Phila Pa 1976) 2008;33:1478-83.

11. Modi HN, Hong JY, Mehta SS, et al. Surgical correction and fusion using posterior-only pedicle screw construct for neuropathic scoliosis in patients with cerebral palsy: a three-year follow-up study. Spine (Phila Pa 1976) 2009;34:1167-75.

12. Allen BL Jr. A pictorial guide to the Galveston LRI pelvic fixation technique. Contemp Orthop 1983;7:51-61.

13. Allen BL Jr, Ferguson RL. The Galveston experience with L-rod instrumentation for adolescent idiopathic scoliosis. Clin Orthop Relat Res 1988;(229):59-69.

14. Ilharreborde B, Hoffmann E, Tavakoli S, et al. Intrasacral rod fixation for pediatric long spinal fusion: results of a prospective study with a minimum 5-year follow-up. J Pediatr Orthop 2009;29:594-601.

15. Early S, Mahar A, Oka R, Newton P. Biomechanical comparison of lumbosacral fixation using Luque-Galveston and Colorado II sacropelvic fixation: advantage of using locked proximal fixation. Spine (Phila Pa 1976) 2005;30:1396-401.

16. Berry JL, Stahurski T, Asher MA. Morphometry of the supra sciatic notch intrailiac implant anchor passage. Spine (Phila Pa 1976) 2001;26:E143-8.

17. Peelle MW, Lenke LG, Bridwell KH, Sides B. Comparison of pelvic fixation techniques in neuromuscular spinal deformity correction: Galveston rod versus iliac and lumbosacral screws. Spine (Phila Pa 1976). 2006 Sep 15;31(20):2392-9.

18. Allen BL Jr, Ferguson RL. The Galveston technique of pelvic fixation with L-rod instrumentation of the spine. Spine (Phila Pa 1976) 1984;9:388-94.

19. Tsuchiya K, Bridwell KH, Kuklo TR, Lenke LG, Baldus C. Minimum 5-year analysis of L5-S1 fusion using sacropelvic fixation (bilateral S1 and iliac screws) for spinal deformity. Spine (Phila Pa 1976) 2006;31:303-8.

20. Kuklo TR, Bridwell KH, Lewis SJ, et al. Minimum 2-year analysis of sacropelvic fixation and L5-S1 fusion using S1 and iliac screws. Spine (Phila Pa 1976) 2001;26:1976-83.

21. Lebwohl NH, Cunningham BW, Dmitriev A, et al. Biomechanical comparison of lumbosacral fixation techniques in a calf spine model. Spine (Phila Pa 1976) 2002;27:2312-20.

22. Erickson MA, Oliver T, Baldini T, Bach J. Biomechanical assessment of conventional unit rod fixation versus a unit rod pedicle screw construct: a human cadaver study. Spine (Phila Pa 1976) 2004;29:1314-9.

23. Kebaish KM. Sacropelvic fixation: techniques and complications. Spine (Phila Pa 1976) 2010;35:2245-51.

24. Saer EH 3rd, Winter RB, Lonstein JE. Long scoliosis fusion to the sacrum in adults with nonparalytic scoliosis: an improved method. Spine (Phila Pa 1976) 1990;15:650-3.

25. O'Brien JR, Yu W, Kaufman BE, et al. Biomechanical evaluation of S2 alar-iliac screws: effect of length and quad-cortical purchase as compared with iliac fixation. Spine (Phila Pa 1976) 2013;38:E1250-5.

26. Wu AM, Chi YL, Ni WF, Huang YX. The feasibility and radiological features of sacral alar iliac fixation in an adult population: a 3D imaging study. PeerJ 2016;4:e1587.